Radiated Sound Power from Near-Surface Acoustic Sources

Article *in* Journal of Ship Research · April 2021

DOI: 10.5957/JOSR.04200025

3 authors, including:

Mahmoud Karimi
University of Technology Sydney

Nicole Kessissoglou
UNSW Sydney

Radiated Sound Power from Near-Surface Acoustic Sources

Mahmoud Karimi[1*], Roger Kinns[2], Nicole Kessissoglou[2]

[1]Centre for Audio, Acoustics and Vibration, University of Technology Sydney, Sydney, Australia

[2]School of Mechanical and Manufacturing Engineering, The University of New South Wales, Sydney, Australia

Abstract

This paper investigates the radiated sound power from idealized propeller noise sources, characterized by elemental monopole and dipole acoustic sources near the sea surface. The free surface of the sea is modelled as a pressure-release surface. The ratio of sound power of the near surface sources to the sound power from the same sources in an unbounded fluid is presented as a function of source immersion relative to sound wavelength. We herein show that the sound power radiated by submerged monopole and horizontal dipole sources is greatly reduced by the effect of the free surface at typical blade passing frequencies. In contrast, the sound power from a submerged vertical dipole is doubled. A transition frequency for the submerged monopole and horizontal dipole is identified. Above this transition frequency, the radiated power is not significantly influenced by the sea surface. Directivity patterns for the acoustic sources are also presented.

Keywords: underwater noise, propeller noise, near-surface sources, monopole sources, dipole sources

[1]Corresponding author: Mahmoud.Karimi@uts.edu.au

1. Introduction

The principal sources contributing to underwater radiated noise (URN) over a wide frequency range are propellers and onboard machinery (Urick, 1983; Ross, 1987; Collier, 1997; Carlton, 2007). Propeller sources are highly complex, but simplification is possible at low frequencies where the wavelength of underwater sound is much larger than propeller dimensions. The propeller may then be regarded as a set of fluctuating forces at the propeller hub and a stationary monopole source that represents the growth and collapse of a cavitation region as each blade passes through the region of wake deficit. This type of model was used by Kinns and Bloor (2004) to examine the net fluctuating forces on a cruise ship hull due to defined propeller sources. The nature of the monopole source was considered by Gray and Greeley (1980), who focused on single screw merchant ships where cavitation is dominant at operational speeds. Non-uniformity in the wake, as well as static pressure that falls towards the sea surface, causes this monopole source to be located near top dead center, closer to the surface than the propeller hub. It introduces cyclic components at multiples of propeller blade passing frequency (bpf) as well as broadband noise over a wide frequency range. These components create a pressure field that acts on nearby hull surfaces, but the URN is controlled by the presence of the pressure release surface that corresponds to the free surface of the sea. The aim of this paper is to investigate how idealized propeller noise sources are influenced by the surface of the sea.

Fluctuating propeller forces are primarily caused by rotation of the propeller in a non-uniform wake. The integrated fluctuating forces on propeller blades radiate sound directly into the sea as dipole sources located at the hub (Carlton, 2007). They are also transmitted to the hull via the local pressure field and via the hub to the thrust block and support bearings (Kinns and Bloor, 2004). As ship speed increases, propeller noise becomes the dominant cause of URN due to the offset of cavitation. Cavitation leads to monopole sources having high radiation efficiency.

The surface of the sea is known to have a fundamental effect on sound radiation from submerged monopole sources arising from propeller cavitation. It is generally assumed that the sea surface is perfectly flat (Ainslie, 2010). Lloyd Mirror corrections are included in noise ranging results and can also be used to estimate cavitation behaviour in existing ships (Carey, 2009). Lloyd Mirror formulae have also been used in both detailed and simplified forms to determine the effect of the sea surface on URN at different declinations and distances from surface vessels (Gray and Greeley, 1980; Arveson and Vendittis, 2000; Gassmann et al., 2017).

To simulate flow around a marine propeller and predict propeller noise, computational fluid dynamics (CFD) coupled with an acoustic analogy is generally employed, for example, see (Kehr and Kao, 2004; Seol, Suh and Lee, 2005; Testa, Ianniello, Salvatore and Gennaretti, 2008; Kellett, Turan and Incecik, 2013) and references therein. Kellett et al. (2013) combined an unsteady Reynolds-averaged Navier Stokes hydrodynamic prediction approach with the Ffowcs Williams and Hawkings equation to study marine propeller noise. The flow around the propeller was simulated using a moving mesh in the CFD domain, considering the ship hull as a rigid surface and the sea free surface as an air-water interface boundary condition. It was shown that at higher frequencies, the effect of the free surface on the radiated noise can be neglected. However at low frequencies, the free surface was found to have a significant impact on noise levels.

The motivation of the current work is to present insight into fundamental results for near surface monopoles and dipoles. Results are presented primarily as sound power radiated by the submerged elemental acoustic sources relative to the power radiated by the same sources in an unbounded fluid. Sound power is examined as a function of ratio of source depth to the wavelength of underwater sound. It is demonstrated that the radiated sound power from submerged vertical dipoles increases at low frequencies by the presence of the sea surface, while it is reduced for monopoles and horizontal dipoles. It is also shown that the radiated power is not influenced significantly by the surface at frequencies above a transition frequency which is identified for submerged monopole and horizontal dipole. Directivity patterns for monopole and dipole sources for selected ratios of source depth to wavelength are presented. Limiting functions for the directivity of the submerged monopole and dipole sources at higher frequencies are also derived. Finally, sound pressure levels for a submerged monopole at different declination angles, below and above its transition frequency, are compared with results for a near surface monopole using Lloyd mirror expressions.

2. The effect of hull excitation

Acoustic sources at the propeller location cause forces to be transmitted to the hull via the propeller shaft and also via the pressure field on the hull surface. This excitation causes hull vibration, which is a principal concern in design of ships such as cruise liners and ferries where passenger comfort is an important consideration. Some of the methods that are used to estimate this hull excitation are described by Breslin and Andersen (1994). The underwater noise due to this hull excitation depends on the hull shape and propeller locations. Its importance relative to direct radiation from propeller sources depends on the proximity of hard hull surfaces relative to the sea surface and will tend to be larger for ships like cruise liners than for frigates which have smaller hull dimensions for similarly sized propellers.

The nature of hull excitation via the pressure field was considered by Kinns and Bloor (2004). They showed how the pressure fields due to monopole and dipole sources in different directions lead to vertical forces on the hull. These vertical forces are the principal cause of sound radiation from the hull at low frequencies. They lead to an array of vertical dipoles, having the cosine directionality that is observed for sources such as propulsion diesel engines as well as propellers. The directionality is the same as for a submerged monopole when only the free surface is considered. Kinns and Bloor (2004) presented the cumulative forces on the hull surface of a twin-screw cruise liner due to different sources at a propeller, where the total force is derived by integration along the

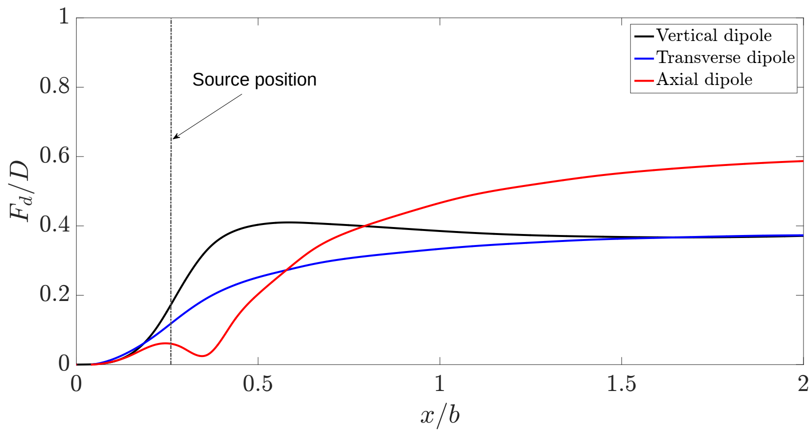

Figure 1: Fluctuating forces (F_d) on the hull surface relative to dipole strength (D) for a cruise liner hull for $kb = 1.62$. b is the beam of the ship and x is a distance from the stern of the ship Kinns and Bloor (2004).

length of the hull, taking relative phase into account. Fig. 1 shows a typical result from that paper, where dimensions are scaled by the beam and the vertical hull force is scaled by the dipole strength. The dipole directions are vertical, transverse and axial (fore-aft). The wavenumber k corresponds to maximum bpf. The vertical dipole leads to a concentrated force near the propeller, but the axial force leads to vertical forces that are further forward. The vertical force transmitted by propeller shaft bearings is the other potentially significant source of underwater noise at low frequencies, which acts in opposition to the forces on the hull surface. The net effect is that vertical hull forces, which may arise from axial and transverse, as well as vertical fluctuating forces at the propeller, are the dominant cause of underwater noise at low frequencies.

The effect of these hull forces is smaller in the case of ship like a frigate, where propellers are closer to the stern and larger in relation to hull dimensions. The remainder of this paper is devoted to the limiting case where the pressure-release surface is the dominant boundary condition and direct sound radiation from submerged sources is the principal cause of underwater radiated noise due to propellers.

3. Sound power from near-surface monopole and dipole sources

Propeller noise becomes dominant at high speeds due to the onset of cavitation (Gray and Greeley, 1980). Cavitation, which leads to monopole sources having high radiation efficiency, is strongly dependent on ship speed. It causes prominent tonals at multiples of propeller bpf and broadband random noise over a wide frequency range (Arveson and Vendittis, 2000). The free surface of the sea is herein considered a perfect pressure release surface. The effect of the free surface on a submerged monopole source is represented by a combination of the source below the surface at depth h and an image of opposite sign at the same distance h above the surface of the sea as shown in Fig. 2. The acoustic power of the submerged monopole can be obtained by integrating the radial intensity over a hemispherical surface with radius of R. Assuming that $R >> h$, the ratio of sound power from a submerged monopole to the sound power from the same unbounded source is given by (Ross, 1987)

$$\frac{W_{\mathrm{m,submerged}}}{W_{\mathrm{m}}} = 1 - \frac{\sin(2kh)}{2kh}. \tag{1}$$

where W_{m} is the the sound power radiated by a monopole in an unbounded space and is given by (Ross, 1987; Pierce, 2019)

$$W_{\mathrm{m}} = \frac{\omega^2 Q^2}{8\pi\rho_f c_f}. \tag{2}$$

where ω is angular frequency, ρ_f is the density of the fluid and c_f is the speed of sound in the fluid. $k = \omega/c_f$ is the acoustic wavenumber and Q is the mass flux amplitude.

The effect of the free surface on the sound power radiated by submerged doublet sources is now considered. A doublet comprises two equal monopole sources, each of mass flux amplitude Q, separated by distance d and in antiphase with each other. At low frequencies, the sound field due to the doublet reduces to that due to a dipole of source strength D if $D = Qd$. At high frequencies, the doublet in an unbounded space radiates the same power as two independent monopoles. Consider submerged horizontal and vertical doublet sources and their image sources as shown in Fig. 2. Assuming $R >> h$ and $R >> d$, the

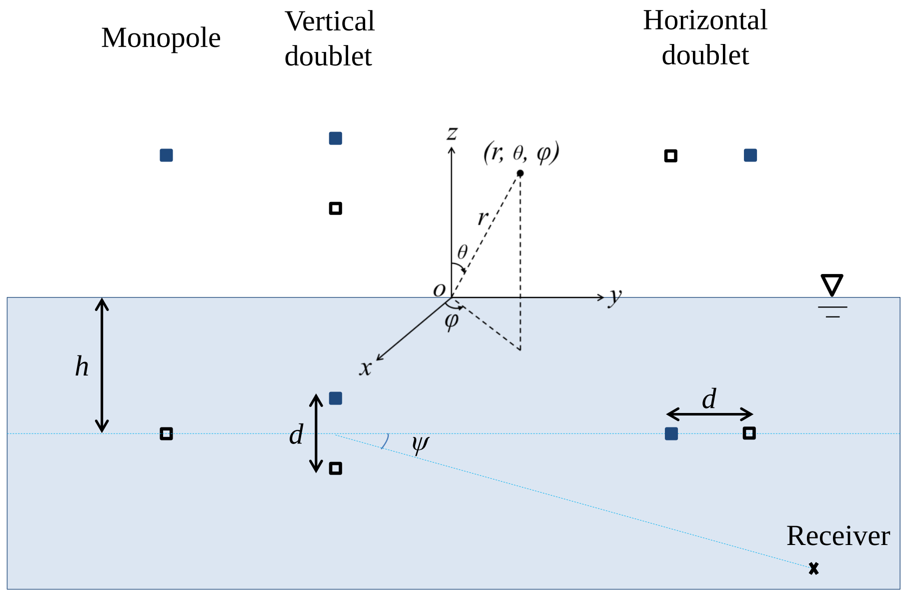

Figure 2: Schematic diagram of submerged monopole, horizontal and vertical doublets.

ratio of acoustic power of the submerged horizontal doublet to the sound power from a dipole in an unbounded space can be written as

$$\left(\frac{W_{\mathrm{db,submerged}}}{W_{\mathrm{dp}}}\right)_{\mathrm{horizontal}} = \frac{12}{\pi k^2 d^2}\int_0^{\pi/2}\int_0^{2\pi}\cos^2(kh\cos\theta)\sin^2(kd\sin\theta\sin\varphi/2)\sin\theta d\varphi d\theta = \frac{12}{k^2d^2}\int_0^{\pi/2}\sin\theta\cos^2(hk\cos\theta)(1-J_0(dk\sin\theta))\,d\theta. \tag{3}$$

where J_0 is the Bessel function of first kind. The ratio of acoustic power of the submerged vertical doublet to the sound power from a dipole in an unbounded space can also be written as

$$\left(\frac{W_{\mathrm{db,submerged}}}{W_{\mathrm{dp}}}\right)_{\mathrm{vertical}} = \frac{24}{k^2 d^2}\int_0^{\pi/2}\cos^2(kh\cos\theta)\sin^2(kd\cos\theta/2)\sin\theta d\theta = \frac{3}{k^2d^2}\left(-\frac{\sin(dk+2hk)}{dk+2hk}-\frac{\sin(kd-2hk)}{dk-2hk}-\frac{2\sin(dk)}{dk}+\frac{\sin(2hk)}{hk}+2\right), \tag{4}$$

where W_{dp} is the sound power radiated by a dipole in an unbounded space and is given by (Ross, 1987)

$$W_{\mathrm{dp}} = \frac{\omega^4 D^2}{24\pi\rho_f c_f^3}. \tag{5}$$

Fig. 3 presents the sound power radiated by a submerged doublet with strength Qd in the horizontal and vertical directions relative to the sound power radiated by a dipole with strength D in an unbounded fluid, for different values of d/h. At low frequencies (small h/λ), the characteristics of the submerged horizontal and vertical doublets are markedly different. The submerged horizontal doublet behaves as a lateral quadrupole up to $h/\lambda \approx 0.25$. The sound power radiated by the submerged vertical doublet is twice that radiated by a dipole in an unbounded space for $h/\lambda < 0.04$ and has a local minimum at $h/\lambda \approx 0.3$. Results for a submerged doublet in any direction converge to results for a submerged dipole over progressively wider ranges of h/λ as d/h is reduced, and ultimately become results for a submerged dipole over the whole range of h/λ. If $kd <<$ 1, the doublets become dipoles. As such, the ratio of sound power from the submerged dipoles to the sound power radiated by a dipole in an unbounded space can now be written as (Skudrzyk, 1971; Ingard and Lamb Jr, 1957)

$$\left(\frac{W_{\mathrm{dp,submerged}}}{W_{\mathrm{dp}}}\right)_{\mathrm{horizontal}} = 3\int_0^{\pi/2} \sin^2(kh\sin\theta)\cos^3\theta d\theta = 1 + \frac{3\cos(2kh)}{(2kh)^2} - \frac{3\sin(2kh)}{(2kh)^3}, \tag{6}$$

$$\left(\frac{W_{\mathrm{dp,submerged}}}{W_{\mathrm{dp}}}\right)_{\mathrm{vertical}} = 6\int_0^{\pi/2} \cos^2(kh\cos\theta)\cos^2\theta\sin\theta d\theta = 1 + \frac{6\cos(2kh)}{(2kh)^2} + \frac{(3(2kh)^2 - 6)\sin(2kh)}{(2kh)^3}. \tag{7}$$

Many surface ships, including ferries, cruise ships, research ships and combat ships, have twin propeller shafts supported by external brackets. Others have podded electric motors with propellers in tractor configurations. Cavitation inception speeds are tending to increase, so that the nature of noise sources below cavitation inception is becoming more significant for surface ships. Dipole sources, extending from very low frequencies to higher frequencies associated with turbulent flow over propeller blades, are potentially significant. These

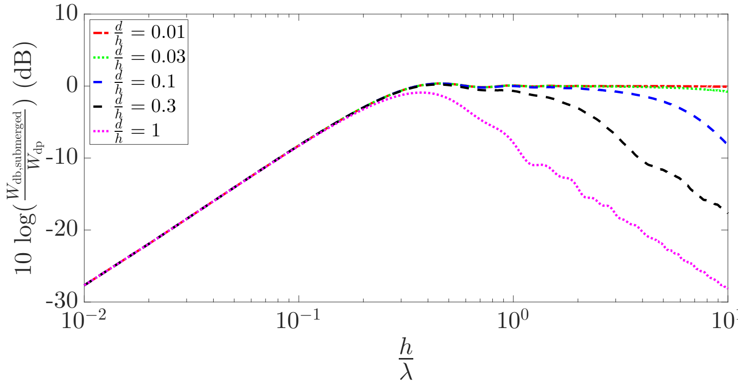

(a)

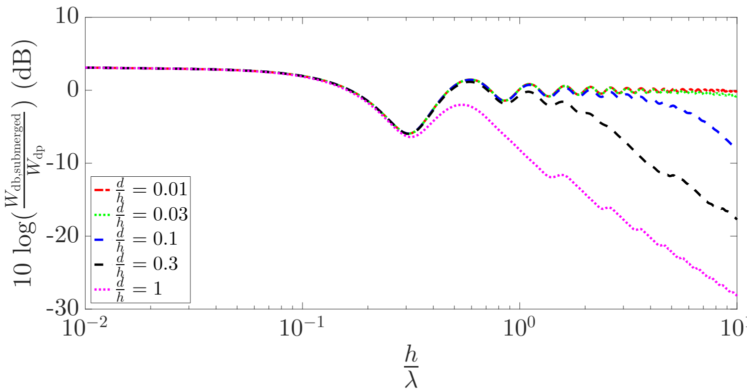

(b)

Figure 3: Sound power radiated by a submerged doublet relative to dipole power in an unbounded fluid, (a) horizontal doublet and (b) vertical doublet.

sources are close to the sea surface, so their sound radiation characteristics, and especially their radiated sound power, are modified by the effects of a nearby pressure-release surface. Additional dipole sources may arise from propeller vibration. Fig. 4 presents results for the near-surface monopole and dipoles using Eqs. (1), (6) and (7). At low frequencies, the sound power of a submerged vertical dipole is double that of a dipole in an unbounded space, as discussed previously. Submerged horizontal dipole sources have the radiation characteristics of a lateral quadrupole in an unbounded space. At $h/\lambda \approx 0.04$, which is close to the usual maximum value of h/λ at propeller blade passing frequency, the sound power radiated by a submerged vertical dipole is about 18 dB greater than for a submerged horizontal dipole. This has important implications for sound radiation from surface ship propellers at bpf and suggests that to minimise URN at bpf below cavitation inception speed, particular attention should be paid to minimization of vertical fluctuating forces. At higher frequencies ($h/\lambda > 1$), the sound power of a submerged source in any direction is unaffected by the sea surface.

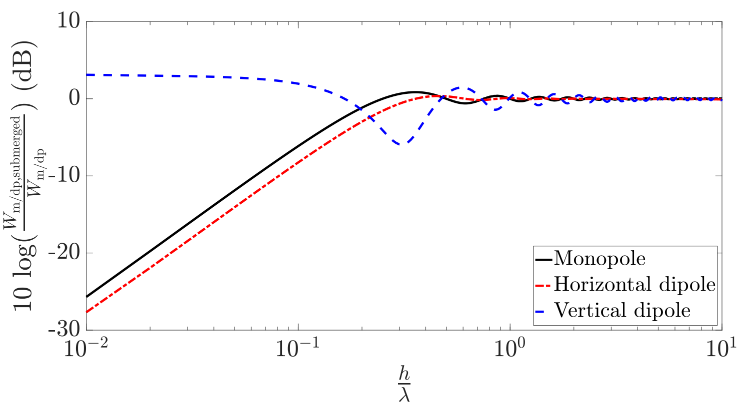

Figure 4: Sound power radiated by submerged monopole and dipole sources relative to the power in an unbounded fluid.

At low frequencies, a vertical dipole at the surface is introduced due to the image source of a submerged monopole. Hence, when $h/\lambda << 1$, the sound power radiated by the submerged monopole is half the radiated power due to a dipole in an unbounded space of source strength $D = Qd$ and spacing $d = 2h$, that is (Ross, 1987)

$$W_{\mathrm{m,submerged}} = \frac{\omega^4 h^2 Q^2}{12\pi\rho_f c_f^3}. \tag{8}$$

We herein identify a transition frequency f_t for each acoustic source above which

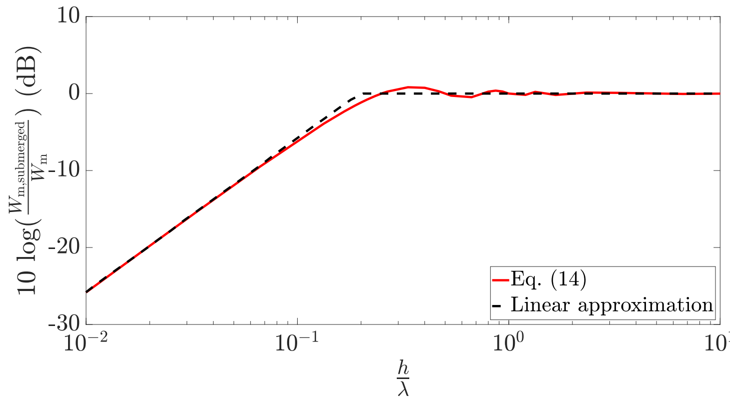

Figure 5: Sound power radiated by a submerged monopole relative to monopole power in an unbounded fluid, compared with the linear approximation given in Table 1.

the radiated sound power is not significantly affected by the sea surface. The sound power radiated by the submerged monopole given by Eq. (8) is equated to the sound power in an unbounded space given by Eq. (2), which yields

$$f_t = \frac{c_f\sqrt{3}}{\pi h\sqrt{8}}, \quad \text{or} \quad \frac{h}{\lambda_t} = \frac{\sqrt{3}}{\pi\sqrt{8}} = 0.195, \tag{9}$$

where λ_t is the wavelength of underwater sound at the transition frequency. Similarly, the transition frequency can be derived for a submerged horizontal dipole. At low frequencies when $h/\lambda << 1$, Eq. (6) can be further simplified to

$$\left(\frac{W_{\mathrm{dp,submerged}}}{W_{\mathrm{dp}}}\right)_{\mathrm{horizontal}} = \frac{2(kh)^2}{5}, \tag{10}$$

To obtain the transition frequency for a submerged horizontal dipole, Eq. (10) is equated to unity (high frequency limit), which yields

$$f_t = \frac{c_f\sqrt{5}}{\pi h\sqrt{8}}, \quad \text{or} \quad \frac{h}{\lambda_t} = \frac{\sqrt{5}}{\pi\sqrt{8}} = 0.252. \tag{11}$$

The ratio of sound power radiated by a submerged monopole/dipole to the sound power radiated from an unbounded monopole/dipole in low and high frequency regimes is presented in Table 1 for each type of source. There is a well-defined transition frequency between these two regimes for the monopole and the horizontal dipole. The maximum error is 1.5 dB if the low frequency formula is used below the transition frequency and the ratio is assumed to be unity above it. For the vertical dipole, there is a gap between the low frequency regime where the sound power is doubled and the high frequency regime where the ratio is unity. The maximum error can exceed 1.5 dB in this gap.

Fig. 5 compares results for the sound power radiated by a submerged monopole using the expression given by Eq. (1) with the low and high frequency approximations listed in Table 1. Results are presented as a function of source depth h relative to the sound wavelength λ. It demonstrates the close agreement between results obtained using the exact and approximate solutions near the transition frequency.

Table 1. Simplified formulae for submerged monopole and dipoles using transition frequencies.

Source type	Low frequency $\frac{W_{\mathrm{m/dp,submerged}}}{W_{\mathrm{m/dp}}}$	Validity h/λ	Transition frequency	High frequency $\frac{W_{\mathrm{m/dp,submerged}}}{W_{\mathrm{m/dp}}}$	Validity h/λ
Monopole	$\frac{8(\pi f h)^2}{3c_f^2}$	< 0.195	$\frac{c_f\sqrt{3}}{\pi h\sqrt{8}}$	1	> 0.195
Horizontal dipole	$\frac{8(\pi f h)^2}{5c_f^2}$	< 0.252	$\frac{c_f\sqrt{5}}{\pi h\sqrt{8}}$	1	> 0.252
Vertical dipole	2	< 0.112	–	1	> 0.426

4. Directivity of near-surface monopole and dipole sources

The directivity of a submerged source at a distance R is herein shown to depend strongly on the type of source, source depth and wavelength of sound. The directivity of submerged monopole and dipole sources can be derived as follows (Ross, 1987)

$$\|p_{\mathrm{m,submerged}}\| = \frac{\omega Q \,\|\sin(kh\sin\psi)\|}{4\pi R}, \tag{12}$$

$$\|p_{\mathrm{dp,submerged}}\|_{\mathrm{horizontal}} = \frac{\omega^2 D \,\|\cos\psi\sin(kh\sin\psi)\cos\varphi\|}{2\pi R c_f}, \tag{13}$$

$$\|p_{\mathrm{dp,submerged}}\|_{\mathrm{vertical}} = \frac{\omega^2 D \,\|\sin\psi\cos(kh\sin\psi)\|}{2\pi R c_f}, \tag{14}$$

where p is acoustic pressure and ψ is the angle between the sea surface and the direction of radiation.

Fig. 6 presents the directivity of the submerged monopole in non-dimensional form $(4\pi R \left\| p_{\mathrm{m,submerged}} \right\| / (\omega Q))$ for selected values of h/λ. The directivity is almost exactly that due to a vertical dipole for $h/\lambda < 0.2$, but the field is notably distorted for $h/\lambda = 0.3$ and exhibits an increasing number of lobes as h/λ is further increased. Fig. 7 presents the directivity patterns for the submerged

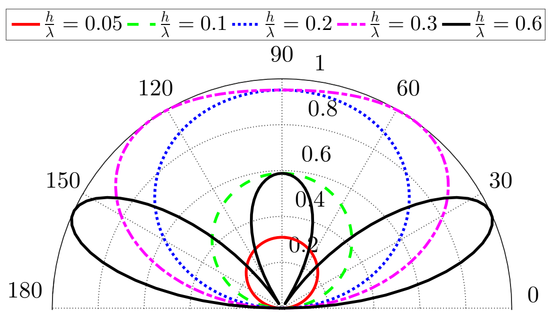

Figure 6: Directivity of the submerged monopole in the vertical plane containing the source for different h/λ.

horizontal dipole in non-dimensional form $(2\pi R c_f \left\| p_{\mathrm{dp,submerged}} \right\| / (\omega^2 D))$ for selected values of h/λ. These patterns are in the vertical plane containing the dipole axis. Their amplitude varies with azimuth as $\cos\varphi$, where φ is zero in the dipole axis direction. Thus, the radiation is zero in the normal vertical plane. The directivity has the pattern associated with a quadrupole for $h/\lambda < 0.2$, but becomes progressively more complex when h/λ increases further. As with the submerged monopole source, the radiated sound power from the submerged horizontal dipole for $h/\lambda > 0.5$ is redistributed but not modified significantly compared to the dipole power in an unbounded fluid. Fig. 8 shows directivity patterns for the submerged vertical dipole, which is equivalent to a vertical fluctuating force. The submerged vertical dipole has similar directivity to the submerged monopole for $h/\lambda < 0.1$, but there is notable distortion for $h/\lambda = 0.2$. There is a significant change in directivity as well as a reduction in

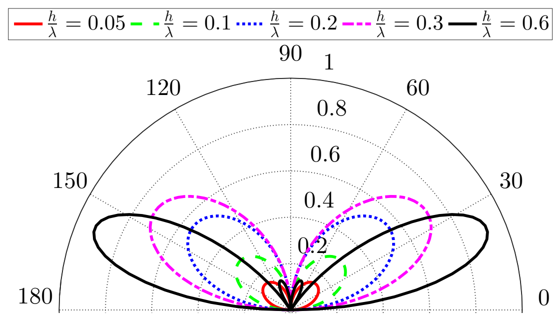

Figure 7: Directivity of the submerged horizontal dipole in the vertical plane containing the source axis for different h/λ.

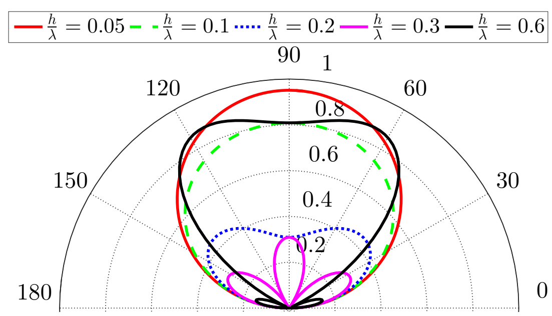

Figure 8: Directivity of the submerged vertical dipole in the vertical plane containing the source axis for different h/λ.

amplitude near $h/\lambda = 0.3$ which is also reflected in Fig. 3(b), showing a 6 dB drop in radiated sound power relative to dipole power in an unbounded fluid. The directivity of each type of submerged source exhibits an increasingly large number of lobes as h/λ increases. These lobes become very narrow, so the pressure amplitude changes rapidly with declination angle ψ. Eqs. (15)-(17) present limiting functions for the directivity of the submerged monopole and dipoles, which are invariant with azimuth angle φ for the monopole and vertical dipole, but vary as $\|\cos\varphi\|$ for the horizontal dipole,

$$\|p_{\mathrm{m,submerged}}\|_{\mathrm{limit}} = \frac{\omega Q}{4\pi R}, \tag{15}$$

$$\|p_{\mathrm{dp,submerged}}\|_{\mathrm{horizontal,limit}} = \frac{\omega^2 D \,\|\mathrm{cos}\psi\mathrm{cos}\varphi\|}{2\pi R c_f}, \tag{16}$$

$$\|p_{\mathrm{dp,submerged}}\|_{\mathrm{vertical,limit}} = \frac{\omega^2 D \,\|\mathrm{sin}\psi\|}{2\pi R c_f}. \tag{17}$$

Fig. 9 shows limiting directivity patterns for the submerged monopole, horizontal dipole and vertical dipole obtained using Eqs. (15)-(17), compared with detailed results for $h/\lambda = 10$ obtained using Eqs. (12)-(14). The lobe amplitudes of the rapidly varying pressure lie within the limiting functions. In practice, the multiple lobes in the directivity patterns tend to be smeared out by the effects of surface roughness and variations in range, source depth and receiver depth, as described by Ross (1987).

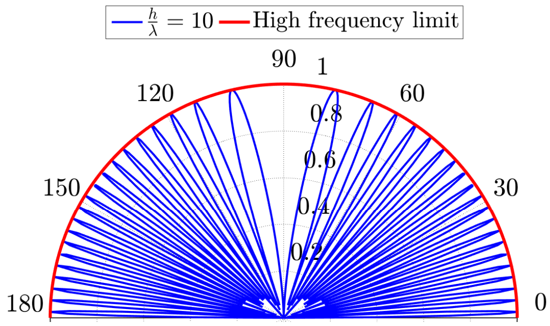

(a)

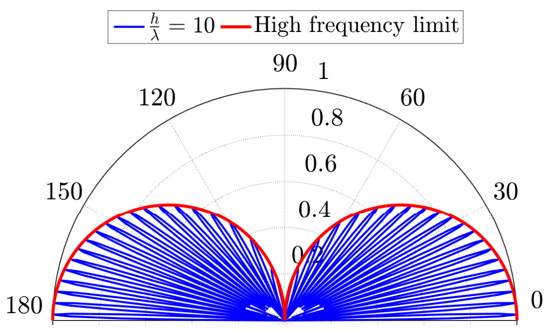

(b)

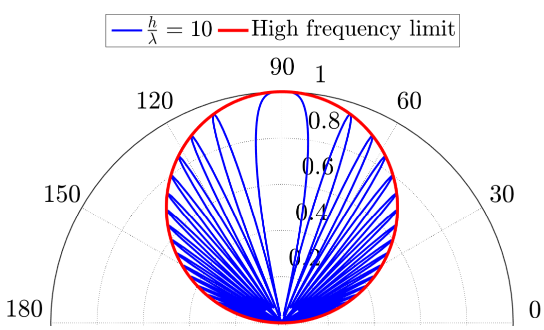

(c)

Figure 9: Limiting directivity of submerged (a) monopole, (b) horizontal dipole and (c) vertical dipole sources compared with the detailed directivity at $h/\lambda = 10$.

5. Sound pressure from a near-surface monopole

The pressures at a receiver position for declination ψ due to a submerged monopole $p_{\mathrm{m,submerged}}$ and a monopole in an unbounded fluid p_{m} are derived in what follows. At high frequencies, $\|p_{\mathrm{m,submerged}}/p_{\mathrm{m}}\|$ oscillates as $\sin(kh\sin\psi)$ owing to successive reinforcement and interference of direct and reflected waves at the receiver. The maximum $p_{\mathrm{m,submerged}} = 2p_{\mathrm{m}}$, so the power-averaged $p_{\mathrm{m,submerged}} = \sqrt{2}p_{\mathrm{m}}$, which is independent of ψ. Thus

$$\left\|\frac{p_{\mathrm{m,submerged}}}{p_{\mathrm{m}}}\right\| \approx \frac{4\pi f h \sin\psi}{c_f}, \qquad f < f_{t,\psi} \tag{18}$$

$$\left\|\frac{p_{\mathrm{m,submerged}}}{p_{\mathrm{m}}}\right\| \approx \sqrt{2}, \qquad f > f_{t,\psi} \tag{19}$$

The transition frequency $f_{t,\psi}$ at a specific declination ψ, where the low and high frequency approximations given by Eqs. (18) and (19) give the same result, can be found as

$$f_{t,\psi} = \frac{c_f}{\pi h \sqrt{8}\sin\psi}. \tag{20}$$

This general approach was used by Kipple (2002) to deduce cruise ship signatures at different ranges. A similar formula to Eq. (20) is given by Wittekind (2014), but his transition frequency is $\pi/\sqrt{8}$ times the value given by Eq. (20). It may be noted that the transition frequency for declination ψ given by Eq. (20) is identical to f_t for sound power given by Eq. (9) if $\sin\psi = 1/\sqrt{3}$, or $\psi = 35°$. This is the angle at which the pressure is the same as the power-averaged pressure over the hemispherical surface.

For a horizontal range of $r_h = 565\,\mathrm{m}$, source depth of $h = 5\,\mathrm{m}$ and declinations of $\psi = 15°$ and $\psi = 45°$ as recently used by Gassmann et al. (2017), Fig. 10 shows predicted Lloyd Mirror behaviour for a near-surface monopole using the following equations (Ross, 1987)

$$\frac{p_{\mathrm{m,submerged}}}{p_{\mathrm{m}}} = 2\sqrt{1-2\beta}\sqrt{\sin^2(\beta k r_b) + \beta^2}, \tag{21}$$

$$\beta = \frac{h h_r}{r_b^2} << 1, \tag{22}$$

$$r_b = \sqrt{h^2 + h_r^2 + r_h^2}, \tag{23}$$

where h_r is the depth of the receiving hydrophone and r_h is the horizontal range from the monopole source to the hydrophone. The results for the linear approximation in Fig. 10 use Eqs. (18) and (19). They agree with the detailed predictions when power averaging over frequency is used to smooth out peaks and nulls at high frequencies (Ross, 1987).

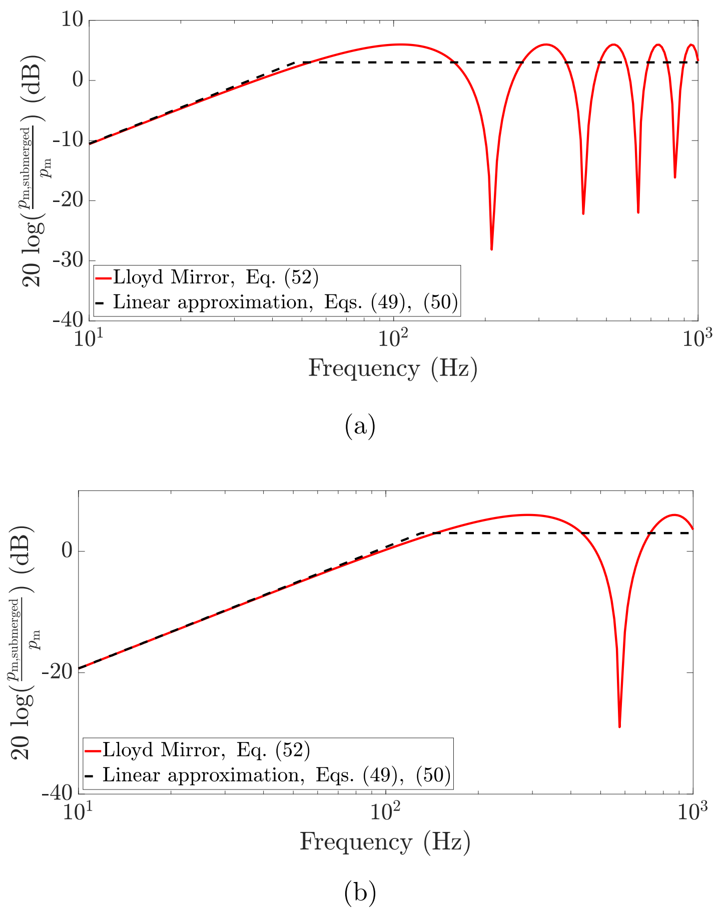

Figure 10: Lloyd Mirror effect for r_h = 565 m range, h=5 m and (a) ψ = 45° hydrophone declination; (b) ψ = 15° hydrophone declination, compared with the linear approximation given by Eqs. (18) and (19).

6. Practical implications

Propeller and hull dimensions vary widely between ship types, but the analysis described in this paper was carried out to underpin design studies for medium to large ships that include frigates, cruise ships and aircraft carriers. Such ships often have twin propellers, using either conventional shaft arrangements or tractor arrangements using submerged pods. Typical propellers might have a diameter $D_p = 5$ meters with 5 blades. Their hubs might be $h = 5$ meters below the surface. Shaft speed is closely proportional to ship speed and might have a typical maximum of 150 rpm, giving a bpf of 12.5 Hz at maximum speed. Thus, $h/\lambda_{bpf} \approx 0.04$. The propeller itself is a compact acoustic source at bpf when $D_p/\lambda_{bpf} \approx 0.04$. Sound radiation at multiples of bpf up to about 5 is often of concern. In this example, the propeller can still be considered to be a compact source over the associated frequency range, but the effect of the free surface on radiated sound power becomes progressively weaker as the transition from low to high frequency behavior is approached.

Blade surface cavitation will tend to occur first as blades approach top dead center, where static pressure is lowest. In this example, where the immersion of the upper proper tip is 2.5 meters, $h/\lambda_{bpf} \approx 0.02$ for the corresponding monopole source and the effect of the free surface extends to higher frequencies. These considerations apply also to random fluctuations in source strengths at low frequencies, which arise from unsteady flow in hull boundary layers and surface waves. These lead to spreading of radiated sound energy over wide frequency ranges. In addition, multiple propellers give rise to interference effects between acoustic sources associated with individual propellers, which can be exploited at multiples of bpf when propeller shaft speeds are constrained to be identical in quiet operation.

During early ship design phases, decisions must be made about the extent of cavitation and magnitude of fluctuating forces that can be accepted in terms of URN requirements at different ship speeds. These requirements are often at specific frequencies, such as multiples of propeller blade passing frequency, and in one-third octave bands. They may be in terms of radiated sound power or radiated noise levels in specific directions. Initially, the hull and propeller designs are undefined. The work described in this paper was carried out to facilitate early stage calculations. The results can be used to check more detailed numerical models and to examine how particular features, such as the nearby hull, surface waves and changes in fluid properties behind a cavitating propeller, modify radiated sound power and directivity.

7. Conclusions

The radiated sound power from submerged monopole and dipole sources relative to the sound power from the same sources in an unbounded fluid has been presented. Far-field radiated noise was calculated using submerged and image sources to represent monopole and doublet behaviour, where the doublet spacing was reduced progressively to derive dipole behaviour associated with radiation due to fluctuating propeller forces. Results show that the dependence of the radiated sound power on source depth relative to sound wavelength varies significantly between submerged monopole sources and dipole sources in vertical and horizontal directions. The nature of noise sources below cavitation inception is becoming more significant for surface ships. Dipole sources, extending from very low frequencies to higher frequencies associated with turbulent flow over propeller blades, are potentially significant. These sources are close to the sea surface, so the sound power they radiate is modified by the effects of a nearby pressure-release surface. The results have significant implications for minimization of underwater radiated noise at multiples of propeller blade passing frequency. Typically, $h/\lambda_{bpf} < 0.04$, so that low multiples of bpf fall in the range $h/\lambda < 0.1$. The radiation due to a vertical fluctuating force is 18 dB greater than that due to a horizontal fluctuating thrust at the same submerged location, if $h/\lambda = 0.04$. This suggests that particular attention should be paid to the reduction of vertical fluctuating forces at multiples of propeller blade passing frequency, if the aim is to minimize underwater noise at these frequencies.

It should be mentioned that the fluctuating forces in different directions at multiples of bpf are often of similar order in quiet twin-screw ship designs, where there is significant cross-flow at the propeller locations. The widely used formulae for surface correction are based on the idea that the ship source can be represented by an equivalent submerged monopole (effectively a vertical dipole at the surface) at low frequencies. This is used to represent the combined effects of cavitation and propeller forces as well as of internal machinery that excite the hull. In this work, we studied the case where the propeller diameter and dipole depth are of similar order to the hull dimensions, so the effect of the free surface is dominant. The effect of the hull surface is likely to become progressively more important when propellers move closer to the hull and more forward of the stern. This will modify the vertical dipole strength for a given vertical force at the propeller. The results in this paper exposed the underlying relationship between disturbing forces and URN and provided the basis for interpretation of results from more complex models.

References

Ainslie, M.A., 2010. Principles of sonar performance modelling. Berlin: Springer.

Arveson, P.T., Vendittis, D.J., 2000. Radiated noise characteristics of a modern cargo ship. J. Acoust. Soc. Am. 107, 118–129.

Breslin, J., Andersen, P., 1994. Hydrodynamics of ship propellers. Cambridge University Press, Cambridge, UK.

Carey, W.M., 2009. Lloyd's mirror-image interference effects. Acoust. Today 5, 14–20.

Carlton, J., 2007. Marine Propellers and Propulsion. 2nd ed., Butterworth-Heinemann.

Collier, R., 1997. Ship and Platform Noise, Propeller Noise, Ch. 46, Encyclopedia of Acoustics. John Wiley & Sons.

Gassmann, M., Wiggins, S.M., Hildebrand, J.A., 2017. Deep-water measurements of container ship radiated noise signatures and directionality. J. Acoust. Soc. Am. 142, 1563–1574.

Gray, L.M., Greeley, D.S., 1980. Source level model for propeller blade rate radiation for the world's merchant fleet. J. Acoust. Soc. Am 67, 516–522.

Ingard, U., Lamb Jr, G.L., 1957. Effect of a reflecting plane on the power output of sound sources. J. Acoust. Soc. Am. 29, 743–744.

Kehr, Y.Z., Kao, J.H., 2004. Numerical prediction of the blade rate noise induced by marine propellers. J Ship Res 48, 1–14.

Kellett, P., Turan, O., Incecik, A., 2013. A study of numerical ship underwater noise prediction. Ocean Eng 66, 113–120.

Kinns, R., Bloor, C., 2004. Hull vibration excitation due to monopole and dipole propeller sources. J. Sound Vib 270, 951–980.

Kipple, B., 2002. Southeast Alaska cruise ship underwater acoustic noise. Naval Surface Warfare Center, Detachment Bremerton, Technical Report NSWCCD-71-TR-2002/574..

Pierce, A.D., 2019. Acoustics: an introduction to its physical principles and applications. Springer.

Ross, D., 1987. Mechanics of Underwater Noise. Peninsula Publishing, Los Altos, CA.

Seol, H., Suh, J.C., Lee, S., 2005. Development of hybrid method for the prediction of underwater propeller noise. J Sound Vib 288, 345–360.

Skudrzyk, E., 1971. The foundations of acoustics: basic mathematics and basic acoustics. Springer-Verlag.

Testa, C., Ianniello, S., Salvatore, F., Gennaretti, M., 2008. Numerical approaches for hydroacoustic analysis of marine propellers. J Ship Res 52, 57–70.

Urick, R.J., 1983. Principles of underwater sound 3rd edition. Peninsula Publising Los Atlos, California .

Wittekind, D.K., 2014. A simple model for the underwater noise source level of ships. J. Ship Prod. Des 30, 7–14.